DOI: 10.48011/asba.v2i1.1391

# Automatic Design of Robust Controllers for Grid-Tied Inverters based on PSO and Kharitonov's Theorem ⋆

**Caio R. D. Osório**[*,**], **Lucas C. Borin**[*], **Gustavo G. Koch**[*], **Everson Mattos**[*], **Pablo García**[***], **Vinicius F. Montagner**[*]

[*] *Federal University of Santa Maria, RS, Brazil*
[**] *Currently a visiting researcher at the University of Oviedo, Spain.*
[***] *Electrical Engineering Department, University of Oviedo, Spain*
*(e-mail: caio.osorio@gmail.com )*

**Abstract:** This paper provides an offline procedure for automatic tuning of robust PI controllers applied to the control of LCL-filtered grid-tied inverters. A particle swarm optimization algorithm is used to tune the control gains based on an objective function, which encompasses frequency and time domain specifications, a limit for the control signal, together with a theoretical assessment of robust stability, by means of Kharitonov's Theorem. Experimental results based on hardware-in-the-loop are provided, confirming that the proposed procedure leads to controls gains that ensure robust stability and suitable grid-injected currents under uncertain grid impedances, complying with the IEEE 1547 Standard and with superior performance when compared to other design alternatives.

*Keywords:* Grid-tied inverter, LCL filter, Robust control, Kharitonov's theorem, Particle swarm optimization.

## 1. INTRODUCTION

In the scenario of renewable energy systems, a key element is the current control of grid-tied inverters (GTIs), which allows to regulate the power flow between energy sources and the mains (Teodorescu et al., 2011). Moreover, the grid currents must comply with different requirements, such as the limits for harmonic distortion of the IEEE 1547 Standard (IEEE, 2011). Therefore, considering the switched nature of the voltage source inverters, output low-pass filters are usually required to interface with the grid, being the LCL filter topology widely used due to the ability to provide suitable high frequency attenuation with reasonable size of magnetics (Ben Saïd-Romdhane et al., 2017).

A widely used alternative for the current control of GTIs with LCL filters are the grid current feedback with proportional-integral (PI) controllers, implemented in synchronous reference frame (Bao et al., 2013). In this context, one important issue is to deal with the inherent resonance peak of the filter, that must be damped by suitable passive or active strategies in order to achieve a stable operation (Dannehl et al., 2010; Hanif et al., 2014). Combined with the appropriate damping technique, the PI controllers have the advantage of being simple, and designs carried out considering only nominal parameters can ensure good performance under stiff grid conditions and when parametric uncertainties are not significant (Chen et al., 2012). On the other hand, the low frequency gain and the crossover frequency of the system have to be reduced to ensure performance and stability when dealing with uncertain parameters, such as the uncertain grid impedances. Thus, the design becomes more difficult, relying on heuristic choices, which usually demand more time from the control designer in trial and error procedures (Pan et al., 2015).

In this context, metaheuristic algorithms are an alternative for the automatic tune of controllers that must cope with multiple objectives and constraints, specially when the objectives are difficult to be expressed analytically (Deb, 2001; Haupt and Haupt, 2004). Among metaheuristic techniques, one can highlight the particle swarm optimization (PSO), a bio-inspired algorithm with simple computational implementation (Eberhart and Kennedy, 1995). The PSO is based on intelligent swarms of particles, that moves in a search space guided by the minimization of an objective function, without relying on its derivative and with good ability to avoid local minima (Sebtahmadi et al., 2017). The PSO algorithm has been used in the literature to tune PI controllers for GTI applications. For instance, in Althobaiti et al. (2016) and Al-Saedi et al. (2011), online optimization algorithms are used to adapt the control gains, while in Hassan and Abido (2011) and de Oliveira et al. (2016), an offline optimization is used to tune fixed controllers. A common point in these works is not including frequency domain specifications in the objective functions, which are useful criteria, often employed in control design of power converters. In Osório et al. (2019), fixed control gains are tunned by the PSO based on the phase margin and crossover frequency. However, although the results illustrate suitable results against uncertain grid

⋆ This study was financed in part by the Coordenação de Aperfeiçoamento de Pessoal de Nível Superior - Brasil (CAPES/PROEX) - Finance Code 001, INCT-GD, CNPq (465640/2014-1, 160884/2019-5 and 309536/2018-9), CAPES (23038.000776/2017-54), FAPERGS (17/2551-0000517-1), and CAPES-PRINT (88887.465639/2019-00).

inductances, the paper does not include a theoretical certificate of robust stability.

In this direction, assuming that the plant is described by a model whose coefficients are not precisely known, but belong to real intervals, the robust stability under uncertain parameters can be theoretically certified by Kharitonov's Theorem (Bhattacharyya et al., 1995; Bernstein and Haddad, 1990). In the context of power electronics, for instance, Kharitonov's Theorem is used to assess robust stability against circuit parametric uncertainties in Yang et al. (2015) and Hote et al. (2009). Nevertheless, in these previous works, Kharitonov's Theorem has been applied to define the regions of robust stability employed for choosing the control gains, but the use of this tool during the control tuning stage is still worthy of investigation. In this sense, Borin et al. (2020) provides a procedure for robust control design including Kharitonov's Theorem, with experimental validation for permanent magnet synchronous machines.

The main contribution of the present work is a procedure for the automatic tunning of robust PI controllers applied to current control of LCL-filtered GTIs, extending the results in Borin et al. (2020) for a higher order plant model. The procedure is executed offine and combines PSO and Kharitonov's Theorem to cope with multiple practical design constraints and robustness against parametric uncertainties. The resulting PI controllers rely on fixed gains that can be easily implemented, avoiding more complex strategies (e.g. adaptive strategies) and also reducing the time demanded from a control engineer during the design stage. As performance criteria, the proposed PSO algorithm encompass time and frequency domain specifications, such as the deviation from reference values for phase margin and crossover frequency and limits for gain margin, overshoot, steady state error and control signal saturation. The robust stability of the closed-loop systems have a theoretical certificate through Kharitonov's Theorem, which is a sufficient condition that can be tested in a fast way during the optimization, by evaluating the stability of only four polynomials. Experimental results based on hardware-in-the-loop are provided, validating the proposed procedure and also establishing a comparison with the results obtained based on other design alternatives.

## 2. MODELING AND PROBLEM DESCRIPTION

Consider a three-phase inverter connected to the grid through an LCL filter, as shown in Figure 1, where $L_c$ and $L_{g1}$ are the converter-side and grid-side filter inductances, respectively. The filter parasitic resistances are given by $r_c$ and $r_{g1}$, $C_f$ is the filter capacitance and $R_f$ is the damping resistance, in series with the capacitor. The grid is modeled with a background voltage $v_g$, in series with a grid resistance $r_{g2}$ and an uncertain grid impedance $L_{g2}$, lying in a bounded interval whose limits are known.

In the synchronous reference frame, Figure 2 shows the block diagram of the plant, where $L_g = L_{g1} + L_{g2}$, $r_g = r_{g1} + r_{g2}$ and $\omega$ is the grid angular frequency.

Assuming that the three-phase grid voltages are sinusoidal and balanced, they can be neglected at this point

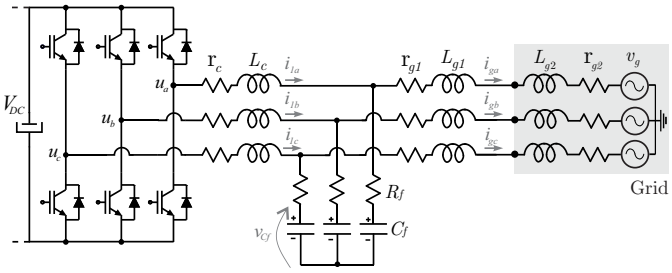


Figure 1. Three-phase grid-tied inverter with LCL filter.

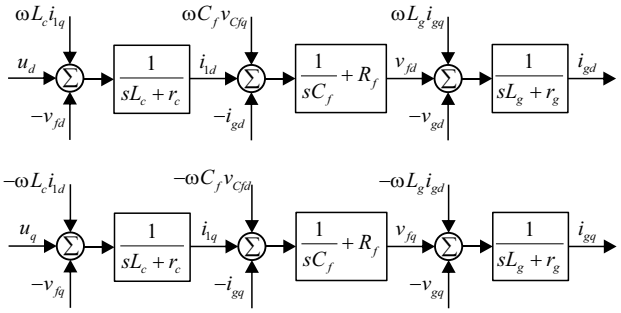


Figure 2. Block diagram of the plant in synchronous reference frame.

(i.e., $v_{gd} = v_{gq} = 0$), being treated as external disturbances (Hanif et al., 2014). Moreover, for the purpose of control design in synchronous reference frame, an usual way to derive the transfer function of the LCL system is to neglect the coupling terms between $d$-axis and $q$-axis, also considering them as external disturbance signals, which greatly simplify the modeling (Xuetao et al., 2015).

Considering the previous assumptions, the transfer function from the inverter output voltage $u(s)$ to the grid-injected current $i_g(s)$, valid for both $d$-axis and $q$-axis, is given by

$$G(s) = \frac{i_g(s)}{u(s)} = \frac{f_1 s + 1}{g_3(L_g)s^3 + g_2(L_g)s^2 + g_1(L_g)s + g_0} \tag{1}$$

where

$$\begin{aligned} f_1 &= C_f R_f, \\ g_3(L_g) &= C_f L_c L_g, \\ g_2(L_g) &= C_f R_f (L_c + L_g) + C_f L_c r_g + C_f L_g r_c, \\ g_1(L_g) &= L_c + L_g + R_f r_g C_f + C_f r_c (R_f + r_g), \\ g_0 &= r_g + r_c \end{aligned} \tag{2}$$

Notice that, due to the uncertainty in the grid inductance $L_{g2}$, the parameter $L_g$ is also uncertain, lying in the interval $[L_{gmin}, L_{gmax}]$. Therefore, $g_3$, $g_2$ and $g_1$ can be written as interval coefficients lying in bounded real intervals, that depend on $L_g$.

In order to control the grid-injected currents, a single-loop grid current feedback control is employed here, for both $d$-axis and $q$-axis, with a PI controller given by

$$C(s) = \frac{K_P s + K_I}{s} \tag{3}$$

with fixed coefficients, defined by the vector

$$c = [K_I \quad K_P] \tag{4}$$

The block diagram of the closed-loop system is shown in Figure 3, for the $d$-axis. To mitigate the effect of the

grid voltage, this disturbance is feedforward in the control action. Also, a compensation decoupling term is included, given by $dec = \omega(L_c + L_g)i_{gq}$, aiming to mitigate the dynamic effect of the inherent coupling between the axes. An analogous block diagram is valid for the $q$-axis.

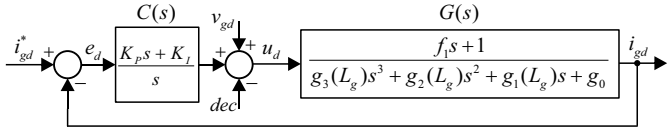


Figure 3. Block diagram of the closed-loop system for the $d$-axis grid current control

It should be noted that the single-loop control method for LCL filters is very susceptible to the resonance peak, being performance and stability highly dependent on the damping of the system. Moreover, the stability and performance are also highly dependent on parameter uncertainties, since the low frequency gain and control bandwidth must be reduced to ensure stability of the system in the entire range of the parameters (Pan et al., 2015; Sivadas and Vasudevan, 2018).

In this context, the control problem to be solved for this case study is to synthesize, with an offline and automatic procedure, fixed gains for the PI controller in (3), that ensure stability and suitable dynamic performance for the entire range of $L_g$.

## 3. ASSESSMENT OF ROBUST STABILITY AND PERFORMANCE

In order to develop an automatic procedure for the tunning of the control gains in (4), it is important to assess the robust stability and performance of the closed-loop system depicted in Figure 3 in a computationally efficient way.

### *3.1 Robust stability based on Kharitonov's Theorem*

Considering a closed-loop system based on a plant subject to uncertain parameters and a controller with fixed control gains, the theoretical robust stability can be easily certified by means of Kharitonov's Theorem.

Given the plant (1), with interval coefficients, and the PI controller (3), the characteristic polynomial of the closed-loop system can be written in the interval form as

$$D(s) = d_0 + d_1 s + d_2 s^2 + d_3 s^3 + d_4 s^4 \tag{5}$$

with coefficients lying in bounded real intervals

$$d_\ell \in \left[ {d_\ell}^-, {d_\ell}^+ \right] \quad , \quad \ell = 0, \cdots, 4 \tag{6}$$

where

$$\begin{array}{l} {d_0}^- = {d_0}^+ = K_I; \\ {d_1}^- = {d_1}^+ = g_0 + f_1 K_I + K_P; , \\ {d_2}^- = g_1(L_{gmin}) + f_1 K_P, \quad {d_2}^+ = g_1(L_{gmax}) + f_1 K_P; \\ {d_3}^- = g_2(L_{gmin}), \quad {d_3}^+ = g_2(L_{gmax}); \\ {d_4}^- = g_3(L_{gmin}), \quad {d_4}^+ = g_2(L_{gmax}). \end{array} \tag{7}$$

According to Kharitonov's Theorem, one has that if the four polynomials (Bhattacharyya et al., 1995)

$$\begin{array}{l} K_1(s) = {d_o}^- + {d_1}^- s + {d_2}^+ s^2 + {d_3}^+ s^3 + {d_4}^- s^4 \\ K_2(s) = {d_o}^- + {d_1}^+ s + {d_2}^+ s^2 + {d_3}^- s^3 + {d_4}^- s^4 \\ K_3(s) = {d_o}^+ + {d_1}^- s + {d_2}^- s^2 + {d_3}^+ s^3 + {d_4}^+ s^4 \\ K_4(s) = {d_o}^+ + {d_1}^+ s + {d_2}^- s^2 + {d_3}^- s^3 + {d_4}^+ s^4 \end{array} \tag{8}$$

are Hurwitz, then $D(s)$ in (5) is Hurwitz and thus, the closed-loop system with control gains $K_P$ and $K_I$ is stable for all values of the $L_g \in [L_{gmin}, L_{gmax}]$.

Therefore, if (8) is satisfied in the scenario specified above, the uncertain closed-loop system will be called from now on, in this paper, as *KT stable*, i.e., stable based on Kharitonov's Theorem.

It should be mentioned that when the coefficients of $D(s)$ in (5) are not independent, i.e., the uncertain parameter $L_g$ appears in more than one coefficient of the transfer function (1) at the same time, then Kharitonov's Theorem tested as in (8) is a sufficient condition for robust stability of the closed-loop system with a given controller (3) (Bhattacharyya et al., 1995). Therefore, although the application of this theorem can lead to conservative results, due to its computational simplicity, it is still worth to be used for a fast evaluation of stability.

### *3.2 Performance criteria based on polytopic representation*

In classical control design procedures for power converters, it is very common to specify performance in terms of frequency domain criteria, such as crossover frequency ($\omega_{co}$), phase margin (PM) and gain margin (GM) (Buso and Mattavelli, 2006; Teodorescu et al., 2011). Moreover, it is also desirable to shape the closed-loop system step response based on time domain performance constraints, such as overshoot (OV) and steady state error ($e_{ss}$). A good trade-off among all these specifications can be a challenge, becoming more difficult when uncertain parameters and control saturation (i.e., a limit for the amplitude of the control signal $u$) must be taken into account in the design stage.

Given a controller with fixed gains, one way to estimate the above performance measures for plants affected by uncertain parameters is from a polytopic representation of the system (Karimi et al., 2007).

Considering the plant (1) and the controller (3), the closed-loop system must be designed to ensure suitable performance against the uncertain parameter $L_g$. By taking into account the extreme values of this parameter, from (1), the resulting polytopic model is limited to 2 vertices, i.e., considering $L_{gmin}$ and $L_{gmax}$. Therefore, the measures of PM, $\omega_{co}$, GM, OV, $e_{ss}$ and the maximum value of $u$ can be carried out evaluating the time and frequency domain responses at these vertices.

Notice that even though the worst case values of the above measures may not be captured by only evaluating the vertices of the polytope, the proposed procedure becomes appealing from the computational point of view, leading to effective results, as will be shown in the sequence.

## 4. PROPOSED CONTROL DESIGN PROCEDURE

In this Section, it is proposed an offline automatic procedure to find the control gains of the PI controller in

(4), such that: a) the closed-loop uncertain system (1) with controller (3) is *KT stable*; b) an objective function including performance specifications in terms of the time and frequency domain criteria is optimized in the vertices of the polytopic model.

To accomplish that, consider the optimization problem

$$c^\star = \arg\min_{c \in \mathcal{C}} \; f(c) \tag{9}$$

where $c^\star$ is the best controller associated with the vector $c$, given in (4), which minimizes the objective function $f(c)$ in a given search space $\mathcal{C}$.

The definition of the objective function, the search space for the gains and the optimization algorithm is given in the sequence.

### *4.1 Objective function*

To measure the quality of the system performance with a given controller candidate $c$, in (4), the objective function proposed here is given by

$$f(c) \;=\; \alpha(c)\;\beta(c)\;\gamma(c) \tag{10}$$

returning a real positive scalar computed based on three terms, $\alpha(c)$, $\beta(c)$ and $\gamma(c)$.

First, assume a reference value $\mathrm{PM}^*$, for the phase margin, and ${\omega_{co}}^*$, for the crossover frequency. Then, the term $\alpha(c)$ is given by

$$\alpha(c) = \max_{j=1,2} \left( \left| \frac{\mathrm{PM}^* - \mathrm{PM}_j(c)}{\mathrm{PM}^*} \right| + \left| \frac{{\omega_{co}}^* - \omega_{coj}(c)}{{\omega_{co}}^*} \right| \right) \tag{11}$$

and measures the worst case deviation of the phase margin and crossover frequency to the respective references. The values of $\mathrm{PM}_j(c)$ and $\omega_{coj}(c)$ are obtained from the transfer function

$$T_j(s) = C(s)G_j(s) \tag{12}$$

which is evaluated for each vertex of the polytopic model, represented by the index $j$, with a given controller candidate $C(s)$, whose coefficients are given by the vector $c$. These values can be easily obtained by means of specialized functions, such as the function *margin*, from MATLAB.

To improve the time and frequency responses, a term $\beta(c)$ is taken into account, including additional constraints to the objective function, such that

$$\beta(c) = \begin{cases} 1, & \begin{array}{l}\text{if } \mathrm{GM}_j(c) \geq \underline{\mathrm{GM}} \text{ and } \mathrm{OV}_j(c) \leq \overline{\mathrm{OV}} \\ \text{and } |e_{ssj}(c)| \leq \overline{e_{ss}} \text{ and } |u_j(c)| \leq \overline{u} \\ \text{for } j = 1, 2\end{array} \\ 10^6, \text{ otherwise} \end{cases} \tag{13}$$

The term $\beta(c)$ returns an unitary value if all the conditions in (13) are satisfied, i.e., if the controller candidate $c$ ensures, for each vertex, compliance with prescribed lower bound $\underline{\mathrm{GM}}$ and upper bounds $\overline{\mathrm{OV}}$, $\overline{e_{ss}}$ and $\overline{u}$. Otherwise, $\beta(c)$ returns the value $10^6$, in order to penalize the objective function for this controller candidate. The indices in (13) can be easily computed, for instance, by means of the functions *margin* and *step*, from MATLAB.

The third term of the proposed objective function, $\gamma(c)$, is related with the robust stability ensured by means of Kharitonov's Theorem, and is given by

$$\gamma(c) = \begin{cases} 1, & \text{if closed-loop system is } \textit{KT stable} \\ 10^6, & \text{otherwise} \end{cases} \tag{14}$$

Note that a positive evaluation of Kharitonov's Theorem is a theoretical guarantee of robust stability for the closed-loop system under uncertain parameter $L_g \in [L_{gmin}, L_{gmax}]$.

It is worth to mention that different objective functions could be defined to guide the control design task. The specifications in (10) were chosen here because, besides considering traditional performance constrains in power electronics (e.g., PM, GM, $\omega_{co}$), they include as a contribution, the robust stability assessment (i.e. *KT stability*) and actuator saturation evaluation in the control design stage.

### *4.2 Search space*

From the definition of the controller coefficients in (4), the space for searching the control gains is given by

$$\mathcal{C} = \begin{cases} (K_I, K_P) \in \mathcal{R}^2 \\ {K_I}^- \leq K_I \leq {K_I}^+, \;\; {K_P}^- \leq K_P \leq {K_P}^+ \end{cases} \tag{15}$$

and is defined here based on the positivity of the coefficients of polynomial (5), for all possible combinations of $L_g \in [L_{gmin}, L_{gmax}]$. This choice is based on the well-known necessary condition for Hurwitz stability. Although it tends to produce a large search space, the advantage is that this space can be systematically obtained in a fast way from a set of linear inequalities, by solving a linear programming problem, and then, including the resulting region in a hyperrectangle, as describe in (15).

Therefore, from (5)–(7), the inequalities used to define the search space are given by

$$\begin{array}{l} K_I > 0 \\ C_f R_f K_P > -(L_c + L_{gmin} + R_f r_g C_f + C_f r_c \left(R_f + r_g\right)) \\ C_f R_f K_I + K_P > -(r_g + r_c) \end{array} \tag{16}$$

where the second inequality is evaluated for $L_{gmin}$ since this condition leads to the more restrictive search space.

It is worth to notice that belonging to this search space is a necessary (but no sufficient) condition to the system stability over the entire range of parameters. More accurate search spaces could be obtained applying, for instance, the complete Routh-Hurwitz criterion, but at the price of more time-consuming and complex calculations to define the search space.

Since $\mathcal{C}$ can be a large search space, exhaustive grid techniques are usually unviable for a high resolution discretization. In this scenario, metaheuristics such as the PSO algorithm has proven to be useful.

### *4.3 Particle swarm optimization*

In the context of the PSO applied to the design problem in this paper, each possible control gain vector $c$, in (4), can be associated with a particle $i$, whose position in the search space is given by

$$s_i = [K_{Ii}, K_{Pi}], \quad i = 1, \cdots, N \tag{17}$$

where $N$ is the number of particles in the swarm.

The particles are randomly initialized on the search space $\mathcal{C}$. In a given epoch $k$, the objective function (10) is evaluated for each particle, based on its position $s_i^k$. The swarm of particles move in the search space from one epoch $k$ to the next epoch $k+1$, until reaching the stop criterion. Therefore, each particle moves from the position $s_i^k$ to the next position $s_i^{k+1}$, with a velocity $v_i^{k+1}$, according to the equations

$$s_i^{k+1} = s_i^k + v_i^{k+1} \quad (18)$$

$$v_i^{k+1} = \lambda v_i^k + \phi_1 r_1 (P_{i.best} - s_i^k) + \phi_2 r_2 (G_{best} - s_i^k) \quad (19)$$

The velocity of a given particle is influenced by the best position that it got ($P_{i.best}$), and also by the best position among all particles of the swarm ($G_{best}$). $\phi_1$ is the cognitive coefficient, $\phi_2$ is the social coefficient, $\lambda$ is the inertia factor and $r_1$ and $r_2$ are random values between $[0, 1]$.

Regarding the configuration of the PSO algorithm, the number of particles $N$ and the coefficients $\phi_1$ and $\phi_2$ are set in order to ensure convergence of the objective function with viable computational effort. The algorithm stop criterion can be set as reaching a maximum number of epochs $M$, or on stalling of the objective function. For instance, using MATLAB, this algorithm can be easily executed using the *particleswarm* function, which present default values for these configurations.

### *4.4 Summary of the proposed procedure*

The proposed design procedure can be summarized by the following steps:

I. Define the system nominal and interval parameters and obtain the plant model (1);
II. Define the control structure and the controller coefficients, as shown in (3) and (4), for the PI controller;
III. Choose the frequency and time domain specifications of the objective function, in (11) and (13);
IV. Based on the characteristic polynomial of the closed-loop system, in (5), determine the search space (15);
V. Set the PSO configurations and run the algorithm.

It is worth to recall that, in each iteration of the PSO, each particle (candidate controller) is evaluated based on the objective function (10), including the assessment of robust stability using Kharitonov's Theorem.

After the execution, if the algorithm converges to a controller $c^\star$ (best particle of the swarm), for which $\beta(c^\star) = 1$ and $\gamma(c^\star) = 1$, all the constraints in (13) are satisfied and the closed-loop robust stability is successfully accessed by Kharitonov's Theorem. Thus, the procedure ends, providing $c^\star$ as a viable robust controller.

If the algorithm converges to a *KT stable* controller, but it is unable to satisfy the constraints in (13), one option is to execute the procedure again, redefining the PSO parameters (for intance, increasing the number of particles and epochs). Alternatively, if necessary, the objective function specifications can be relaxed to obtain a viable controller.

## 5. DESIGN EXAMPLE

Following the first step of the proposed procedure, consider the parameters of the LCL-filtered grid-tied inverter given in Table 1. The parasitic resistances are neglected, and the grid inductance is an uncertain parameter lying in a bounded interval.

Table 1. System parameters

| System description | |
|---|---|
| Switching frequency $f_{sw}$ | 10020 Hz |
| Sampling frequency $f_s$ | 20040 Hz |
| DC-link $V_{dc}$ | 400 V |
| Grid voltage $V_g$ | 220 Vrms, 60 Hz |
| Converter inductance $L_c$ | 1 mH |
| Grid-side inductance $L_{g1}$ | 0.3 mH |
| Filter capacitor $C_f$ | 62 $\mu$F |
| Grid inductance $[L_{g2min}, L_{g2max}]$ | [0.1 1.5] mH |
| Grid resistance $r_g$ | 0.1 $\Omega$ |
| Damping resistance $R_f$ | 1 $\Omega$ |

For the second step, the control structure is defined as the one given in Figure 3, with the PI controller.

The third step in the proposed procedure is to choose the objective function specifications. Thus, the reference values for system performance and stability margins are specified as

$$\begin{array}{lll} \underline{\omega_{co}}^* = 600 \text{ rad/s} & \text{PM}^* = 60^\circ & \underline{\text{GM}} = 5 \ (14 \ dB) \\ \overline{\text{OV}} = 10\% & \overline{e_{ss}} = 0\% & \overline{u} = 1 \end{array} \quad (20)$$

Regarding the step IV, the limits of the search space are defined based on (15) and (16). For simplicity, a rectangular region with $K_P > 0$ and $K_I > 0$ is considered, and the upper bounds are set as $10^4$, in order to have a large region for searching both control gains.

For the last step, the PSO is configured with parameters

$$\text{N} = 200 \text{ particles, M} = 50 \text{ epochs, } \phi_1 = 0.5, \ \phi_2 = 0.5 \quad (21)$$

and the algorithm is executed.

To illustrate the success rate of the results, the algorithm was executed 20 times, having always converged in about 3 minutes to a viable controller with low deviation of the gains among the executions. For a typical execution, the evolution of the best value of $f(c)$ in each epoch (called fitness) is depicted in Figure 4(a), and the control gains are given by

$$c^\star = [K_I \ K_P] = [102.13418 \ \ 0.95822] \quad (22)$$

The closed-loop system in Figure 3 was simulated with the control gains in (22). The step responses of the closed-loop system for the extreme values of grid inductances are shown in Figure 4(b), where the maximum overshoot is $\text{OV}_{max} = 8.88\%$ and there is no error in steady state.

The frequency responses of the open-loop transfer function $T(s) = C(s)G(s)$ is shown in Figure 5, for $L_{gmin}$ and $L_{gmax}$, which confirm system stability for the entire range of parameters. The minimum values of the stability margins and crossover frequency were achieved with $L_{gmax}$, for which $\text{GM}_{min} = 14.1 \ dB$, $\text{PM}_{min} = 79.1^\circ$, $f_{comin} = 56.8$ Hz ($\approx 357$ rad/s). From the results shown in Figures 4 and 5, it is possible to confirm that all constraints in (20) were satisfied.

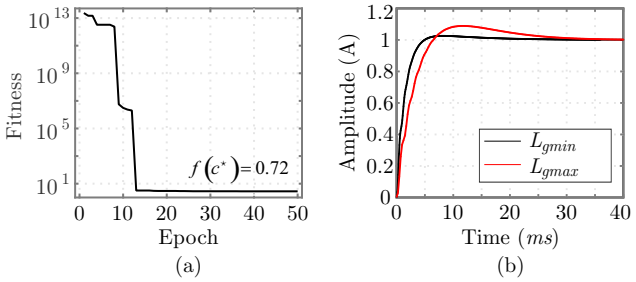


Figure 4. Results for a typical execution: (a) Fitness curve; (b) Step responses with gains (22).

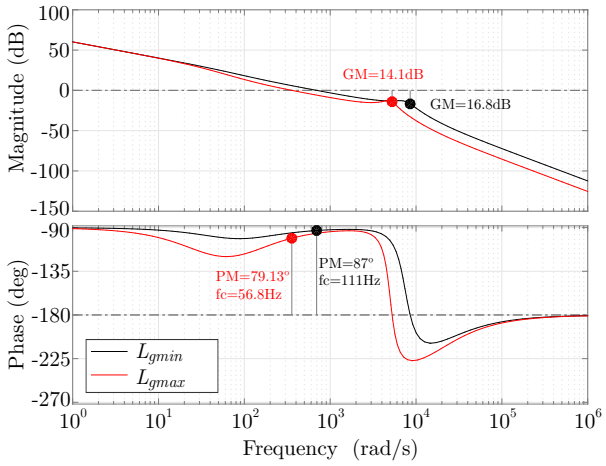


Figure 5. Bode diagrams with gains (22), from $i_{ref}$ to $i_g$.

### *5.1 Experimental Results based on HIL*

Real-time tests based on hardware-in-the-loop (HIL) are presented to validate the control gains designed with the proposed procedure. The LCL-filtered GTI depicted in Figure 1 was emulated with parameters in Table 1, using a Typhoon HIL, model 402.

For the digital implementation, consider the discretization of the PI controller (22) using the Tustin method, with the sampling frequency given in Table 1. The DSP TMS32F28335, from Texas Instruments, is used to implement the controllers, assuming the same gains for both $d$ and $q$ axes, including the feedforward of the grid voltage and also the decoupling terms, as shown in Section 2. The angle for the Park transform (i.e., to obtain the signals in $dq$ coordinates) is obtained using a Kalman Filter algorithm, ensuring that the three-phase grid currents are synchronized with the voltages at the point of common coupling (Cardoso et al., 2008). To drive the inverter switches, a space vector modulation is employed.

Figure 6 shows the grid current responses, in $d$-axis and $q$-axis, for sudden variations in the grid current references, considering the extremes of the uncertain parameter $L_g$. The first variation represents the start-up of the system, injecting active power into the grid, while the second variation represents a transient from active to reactive power. It is possible to verify that, with the PSO-based PI controller, the closed-loop system is able to track the references respecting the performance constraints established in the design and also with suitable settling times, for both grid conditions. The transient responses for $L_{gmax}$

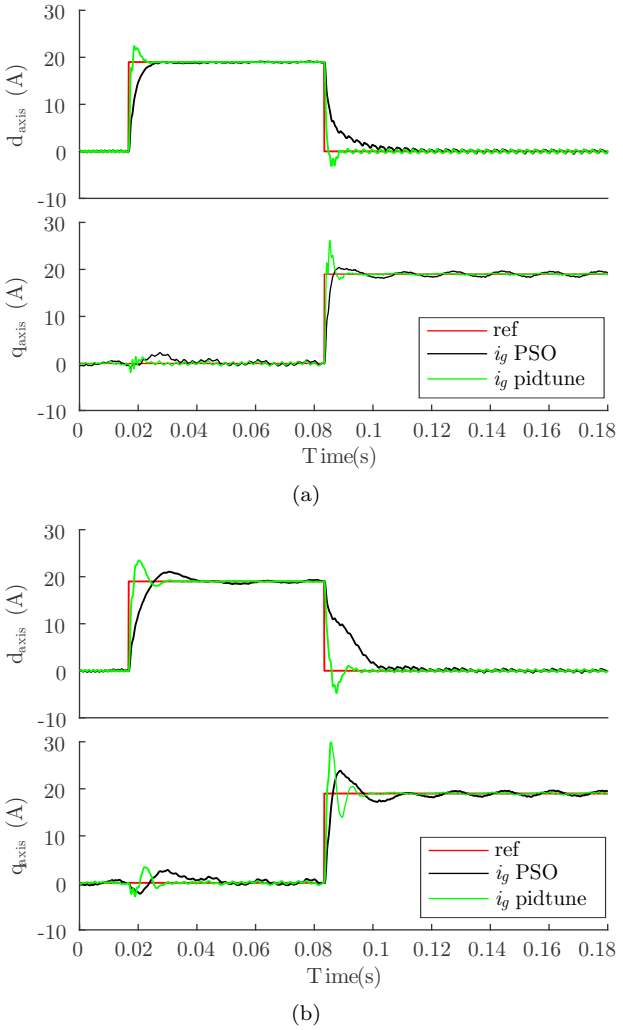


Figure 6. Step responses with the PSO-based and the *pidtune* PI controllers, for: (a) $L_{gmin}$; (b) $L_{gmax}$.

are slower than the responses for $L_{gmin}$, which is expected due to the need of ensuring robustness over the entire range of parameters with a simple fixed gain controller.

In order to establish a comparison between the proposed procedure and an well-known tuning technique, Figure 6 also shows the responses with a PI controller designed using the *pidtune* function, from MATLAB. In this case, the controller was designed for $L_{gmax}$, and considering the same specifications used for the PSO: $\omega_{co}{}^* = 600$ rad/s and $\text{PM}^* = 60°$. It is possible to verify superior performance of the closed-loop system with the PI controller designed based on the proposed procedure. A more detailed performance comparison will be presented in Table 2, in the next section.

For the system operating with the PSO-based controller, the three-phase grid currents with respect to the transient responses presented in Figure 6(a) and (b) are shown in Figure 7(a) and Figure 7(a), respectively. From these results, it is possible to confirm robust stability and suitable transient performances for both extreme values of the grid inductances.

The grid currents in steady-state are highlighted in Figure 8(a), for $L_g = L_{gmin}$, and in Figure 8(b), for $L_g =$

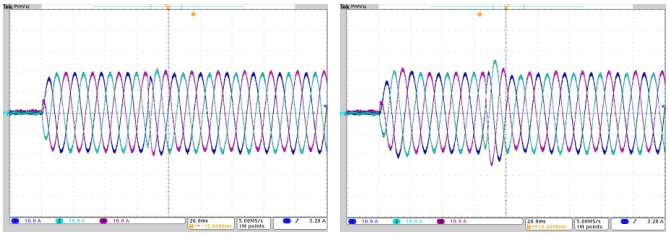

(a) (b)

Figure 7. Transient responses of the three-phase grid currents for the system operating with the PSO-based PI controller and: (a) $L_g = L_{gmin}$; (b) $L_g = L_{gmax}$

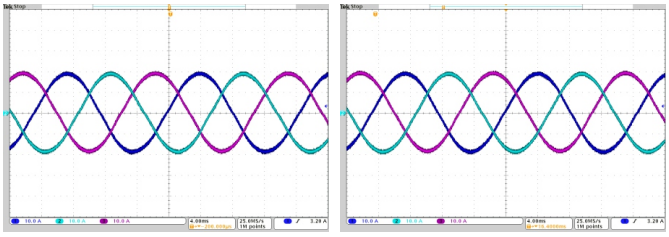

(a) (b)

Figure 8. Three-phase grid currents in steady-state for the system operating with the PSO-based PI controller and: (a) $L_g = L_{gmin}$; (b) $L_g = L_{gmax}$.

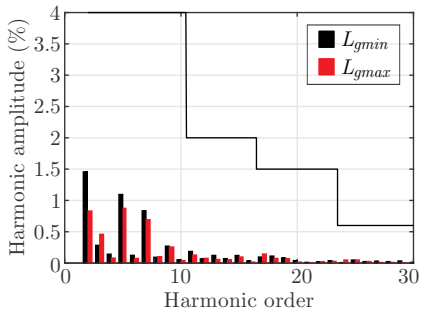


Figure 9. Steady-state responses: current harmonic spectrum and limits from IEEE 1547.

$L_{gmax}$. From these waveforms, Figure 9 shows that the harmonic spectra of the grid currents comply with the requirements of the IEEE 1547 Standard, for both extreme values of $L_g$. Moreover, the total harmonic distortion (THD) is equal to 2.13%, for $L_{gmin}$, and 1.59%, for $L_{gmax}$, also complying with this standard (THD $\leq$ 5%).

## 6. COMPARATIVE ANALYSIS

For a comparative analysis, Table 2 shows performance criteria obtained with controllers designed using the proposed procedure and two other control tunning strategies. The measures given in the Table 2 are the worst case values for each design specification, obtained based on simulations for the vertices of the polytopic model.

First, consider the controller designed using the *pidtune* function, from MATLAB, with experimental results already shown in Figure 6. The measurement of the performance criteria with this controller is better detailed in the second column of Table 2, from which it is possible to verify that it led to acceptable closed-loop responses. On the other hand, in comparison with the proposed PSO-based controller, the performance are inferior in terms of gain margin and overshoot. Moreover, the *pidtune* controllers do not have a theoretical certificate of robust stability under parametric uncertainties and also may lead to control saturation.

In order to provide a comparison between the PSO and a different optimization tool, consider the genetic algorithms (GA), which are a well established metaheuristic that could have been used in the proposed procedure (Haupt and Haupt, 2004). In this sense, a GA is configured here using the same objective function proposed in (10) and with parameters similar to the ones used for the PSO (e.g. same number of particles for PSO and chromosomes for GA, epochs for PSO and generations for GA). Columns 1 and 3 of Table 2 show that both PSO and GA lead to similar results in terms of phase margin, crossover frequency, gain margin and overshoot. On the other hand, a statistical analysis performed when repeating 20 times the execution of both algorithms shows that, in comparison to the GA, the PSO has the advantage of converging, in average, in half the time. Moreover the PSO executions present a higher success rate and a lower dispersion of the solutions. This analysis is summarized in Table 3, confirming that the PSO is a suitable optimization algorithm for the proposed procedure.

To obtain the statistics in Table 3, the success rate was defined by the ratio between the number of successful executions and the total number of executions, where a successful execution is when the algorithm converged to a controller $c^\star$ that has $\beta(c^\star) = 1$ and $\gamma(c^\star) = 1$. The dispersion was defined as the standard deviation of the value $f(c^\star)$ divided by its average value.

Table 2. Design comparisons

| | PSO | Pidtune | GA |
|---|---|---|---|
| PM (deg) | 79.13 | 60.1 | 79.24 |
| $\omega_c$ (rad/s) | 356.88 | 955.04 | 354.75 |
| GM (dB) | 14.1 | 6.34 | 14 |
| OV (%) | 8.88 | 27.0 | 8.75 |
| Saturation | No | Yes | No |
| *KT stable* | Yes | No | Yes |
| $K_P$ | 0.958 | 2.190 | 0.952 |
| $K_I$ | 102.1 | 1300 | 99.99 |

Table 3. Statistics Comparison between GA and PSO Algorithms

| | **PSO** | **GA** |
|---|---|---|
| Success rate | 100% | 60% |
| Dispersion | 0.824% | 4.52% |

## 7. CONCLUSION

This paper proposed a procedure for the automatic tunning of robust PI controllers applied to LCL-filtered GTIs. A PSO algorithm is employed to optimize an objective function for the vertices of a polytope, taking into account important frequency and time-domains criteria. During the optimization, the PSO is capable of finding PI control gains which ensure, for the entire domain of grid impedances, suitable performances and the robust stability

certified by Kharitonov's Theorem. This theorem is used here within the optimization procedure, and not in an a priori fashion to determine the region for the search of the control gains. Experimental results based on HIL confirm that the proposed procedure leads to viable controllers, ensuring robust stability, suitable dynamic performance and compliance with the IEEE 1547 Standard. Therefore, the proposed procedure can be seen as an alternative for automatic tunning of controllers that must cope with multiple specifications, avoiding time-consuming design stages, specially considering robust stability against uncertain parameters.

## REFERENCES


Al-Saedi, W., Lachowicz, S.W., and Habibi, D. (2011). An optimal current control strategy for a three-phase grid-connected photovoltaic system using particle swarm optimization. In *2011 IEEE Power Engineering and Automation Conference*, volume 1, 286–290.

Althobaiti, A., Armstrong, M., and Elgendy, M.A. (2016). Control parameters optimization of a three-phase grid-connected inverter using particle swarm optimisation. In *8th IET International Conference on Power Electronics, Machines and Drives (PEMD 2016)*, 1–6.

Bao, X., Zhuo, F., Tian, Y., and Tan, P. (2013). Simplified feedback linearization control of three-phase photovoltaic inverter with an LCL filter. *IEEE Transactions on Power Electronics*, 28(6), 2739–2752.

Ben Saïd-Romdhane, M., Naouar, M.W., Slama-Belkhodja, I., and Monmasson, E. (2017). Robust active damping methods for LCL filter-based grid-connected converters. *IEEE Transactions on Power Electronics*, 32(9), 6739–6750.

Bernstein, D.S. and Haddad, W.M. (1990). Robust controller synthesis using Kharitonov's theorem. In *29th IEEE Conference on Decision and Control*, 1222–1223.

Bhattacharyya, S.P., Chapellat, H. and Keel, L.H. (1995). *Robust control – the parametric approach*, Prentice Hall PTR.

Borin, L.C., Osório, C.R.D., Koch, G.G., Gabbi, T.S., de Oliveira, R.C.L.F., and Montagner, V.F. (2020). Robust control design procedure based on particle swarm optimization and Kharitonov's theorem with an application for pmsms. *Brazilian Journal of Power Electronics*, 25(2), 219 – 229.

Buso, S. and Mattavelli, P. (2006). *Digital Control in Power Electronics*. Morgan & Claypool Publishers.

Cardoso, R., de Camargo, R.F., Pinheiro, H., and Gründling, H.A. (2008). Kalman filter based synchronisation methods. *IET Generation, Transmission Distribution*, 2(4), 542–555.

Chen, X., Gong, C.Y., Wang, H.Z., and Cheng, L. (2012). Stability analysis of LCL-type grid-connected inverter in weak grid systems. In *2012 International Conference on Renewable Energy Research and Applications*, 1–6.

Dannehl, J., Fuchs, F., Hansen, S., and Thøgersen, P. (2010). Investigation of active damping approaches for PI-based current control of grid-connected pulse width modulation converters with LCL filters. *IEEE Transactions on Industry Applications*, 46(4), 1509 – 1517.

Deb, K. (2001). *Multi-objective optimization using evolutionary algorithms*, volume 16. John Wiley & Sons.

Eberhart, R. and Kennedy, J. (1995). A new optimizer using particle swarm theory. *Proceedings of the Sixth International Symposium on Micro Machine and Human Science.*, 39–43.

Hanif, M., Khadkikar, V., Xiao, W., and Kirtley, J.L. (2014). Two degrees of freedom active damping technique for LCL filter-based grid connected pv systems. *IEEE Transactions on Industrial Electronics*, 61(6), 2795–2803.

Hassan, M.A. and Abido, M.A. (2011). Optimal design of microgrids in autonomous and grid-connected modes using particle swarm optimization. *IEEE Transactions on Power Electronics*, 26(3), 755–769.

Haupt, R. and Haupt, S. (2004). *Practical Genetic Algorithms*. Wiley-Interscience publication. John Wiley.

Hote, Y.V., Choudhury, D.R., and Gupta, J. (2009). Robust stability analysis of the PWM push-pull DC–DC converter. *IEEE transactions on power electronics*, 24(10), 2353–2356.

IEEE (2011). IEEE:1547 standard for interconnecting distributed resources with electric power systems.

Karimi, A., Khatibi, H., and Longchamp, R. (2007). Robust control of polytopic systems by convex optimization. *Automatica*, 43(8), 1395–1402.

Oliveira, F.M., Oliveira da Silva, S.A., Durand, F.R., Sampaio, L.P., Bacon, V.D., and Campanhol, L.B.G. (2016). Grid-tied photovoltaic system based on PSO MPPT technique with active power line conditioning. *IET Power Electronics*, 9(6), 1180–1191.

Osório, C.R.D., Borin, L.C., Koch, G.G., and Montagner, V.F. (2019). Optimization of robust PI controllers for grid-tied inverters. In *2019 IEEE 15th Brazilian Power Electronics Conference and 5th IEEE Southern Power Electronics Conference (COBEP/SPEC)*, 1–6.

Pan, D., Ruan, X., Bao, C., Li, W., and Wang, X. (2015). Optimized controller design for LCL-type grid-connected inverter to achieve high robustness against grid-impedance variation. *IEEE Transactions on Industrial Electronics*, 62(3), 1537–1547.

Sebtahmadi, S.S., Azad, H.B., Kaboli, S.H.A., Islam, M.D., and Mekhilef, S. (2017). A PSO–DQ current control scheme for performance enhancement of Z–source matrix converter to drive IM fed by abnormal voltage. *IEEE Transactions on Power Electronics*, 33(2), 1666–1681.

Sivadas, D. and Vasudevan, K. (2018). Stability analysis of three-loop control for three-phase voltage source inverter interfaced to the grid based on state variable estimation. *IEEE Transactions on Industry Applications*, 54(6), 6508–6518.

Teodorescu, R., Liserre, M., and Rodríguez, P. (2011). *Grid Converters for Photovoltaic and Wind Power Systems*. Wiley - IEEE. John Wiley & Sons.

Xuetao, P., Tiankai, Y., Keqing, Q., Jinbin, Z., Wenqi, L., and Xuhui, C. (2015). Analysis and evaluation of the decoupling control strategies for the design of grid-connected inverter with LCL filter. *International Conference on Renewable Power Generation*, 1–6.

Yang, X., Yuan, Y., Long, Z., Goncalves, J., and Palmer, P.R. (2015). Robust stability analysis of active voltage control for high-power IGBT switching by Kharitonov's theorem. *IEEE Transactions on Power Electronics*, 31(3), 2584–2595.